(C)

2021　2023

Real-time precision functional network mapping of the human brain for neurosurgical applications

Real-time precision functional network mapping of the human brain for neurosurgical applications

BAGARINAO, Epifanio

3,200,000

MRI

FCOR
FCOR
FCOR
FCOR
FCOR

Our results demonstrated the feasibility of using FCOR analysis to extensively evaluate alterations in brain network before and after neurosurgical operations. Real-time construction of FCOR maps could also enable intraoperative assessment of the brain connectome during surgery.

This study aimed to develop a system for the real-time construction of individualized, highly reliable and reproducible connectivity profile of the human brain using resting-state functional MRI for neurosurgical applications. For this, we used functional connectivity overlap ratio (FCOR), a network metric that quantifies a region's functional connections to different large-scale brain networks. Our findings demonstrated the feasibility of constructing whole-brain FCOR maps in real-time. Highly reproducible FCOR maps could also be generated using large fMRI data. FCOR analysis was also successful in identifying connectivity alterations before and after thalamotomy in patients with essential tremor, demonstrating the potential use of FCOR for neurosurgical applications.

precision mapping real-time fMRI functional connectivity essential tremor resting-state f MRI human connectome

１．研究開始当初の背景

Resting-state functional magnetic resonance imaging (fMRI), a well-established MRI technique, has enabled the identification and mapping of "whole-brain networks" (or the brain connectome) that has led to a shift towards the use of "network-centric" approaches in studying brain function and organization. Driven by this paradigm shift, neurological and psychiatric disorders are investigated in terms of alterations in brain networks, advancing further our understanding of these disorders. However, the clinical applications of network-based approaches remain limited. To use these modern, cutting-edge techniques in clinical settings, several important issues must be addressed. These include establishing a comprehensive metric to characterize brain networks, obtaining highly reliable and reproducible estimates of this metric at the individual level, and enabling the immediate estimation of this metric to make it readily accessible even during scanning, which could significantly benefit neurosurgical operations.

２．研究の目的

The primary purpose of this study was to develop a system for the real-time construction of individualized, highly reliable and reproducible connectivity profile of the human brain using resting-state fMRI for neurosurgical applications. Specifically, we aimed to develop a *real-time functional MRI analysis system* to enable the real-time (or online) generation of individual connectivity profile during MRI scans. To characterize the connectivity profile at the voxel level, we used a network metric we recently developed called *functional connectivity overlap ratio* (FCOR) (Bagarinao et al., 2020), which quantifies a voxel's connection to different canonical resting-state networks. In addition, we also examined the use of *precision functional mapping* (Gordon et al., 2017), a technique that involves scanning an individual multiple times, to generate highly reliable and reproducible FCOR maps at the individual level. Finally, as a preliminary investigation, we also examined changes in the connectivity profile (pre- and post-treatment) of patients with essential tremor undergoing MR-guided focused ultrasound (MRgFUS) thalamotomy using individually constructed FCOR maps and identified whether surgical outcomes could be reliably predicted from these changes.

３．研究の方法

(1) Participants

For precision mapping experiment, 20 healthy participants (10 males/10 females, mean age: 23.25 years) were recruited from Nagoya University. All participants underwent two imaging sessions separated by 28.75 days on average. For the experiment investigating changes in connectivity in patients with essential tremor, MRI data from 27 patients (20 males/7 females, mean age: 71.19 years) with essential tremor and 27 age- and sex-matched healthy controls (20 males/7 females, mean age: 70.89 years) were used in this study. Of the 27 patients, 15 patients (11 males/4 females) underwent additional MRI scanning 6.7 ± 1.2 months after MR-guided focused ultrasound (MRgFUS) thalamotomy. Basic information collected from patients included age, sex, disease duration, medication, and cognition, assessed using the Japanese version of Addenbrooke's Cognitive Examination – Revised (ACE-R). The severity of tremor was also assessed using the Clinical Rating Scale for Tremor (CRST) score before and after thalamotomy. This study was approved by the Ethics Committee of Nagoya University Graduate School of Medicine (approval numbers: 2017-0147 & 2021-0238) and all participants provided written informed consent before joining the study.

(2) Magnetic resonance imaging

All participants underwent MRI scans at the Brain and Mind Research Center, Nagoya University using a Siemens Magnetom Verio (Siemens, Erlangen, Germany) 3.0 Tesla MRI scanner with a 32-channel head coil. For the precision mapping study, each scanning session consisted of an anatomical localizer scan, a T1-weighted MRI scan for anatomical reference, and four 15-min resting-state fMRI scans. During resting-state fMRI scans, participants were also given feedback information representing head motion and instructed to minimize head motion using this information. For the study involving essential tremor patients, each imaging session consisted of a T1-weighted MRI scan and an 8-min resting-state fMRI scan.

For offline analysis, the MRI data from all participants were processed using Statistical Parametric Mapping (SPM12, Wellcome Trust Center for Neuroimaging, London, UK) software running on Matlab (R2021, MathWorks, Natick, Mass, USA). The anatomical T1-weighted MRI data were segmented into component images using SPM12's segmentation approach. Biased-corrected T1-weighted images were also generated and the transformation information from subject space to the Montreal Neurological Institute (MNI) template space was obtained. After removing the first five volumes, the resting-state fMRI data were slice-time corrected, realigned, co-registered to the biased-corrected anatomical image, normalized to MNI space, resampled to a $3\times3\times3$ mm^3 voxel resolution, and smoothed using a 6-mm full-width-at-half-maximum Gaussian filter. The preprocessed images were further corrected for the effects of head motion

and other physiological noise. Finally, a bandpass filter within 0.01 – 0.1 Hz was applied.

(3) FCOR analysis

Using the preprocessed resting-state fMRI data, FCOR maps were generated. For the precision mapping study, we used an incremental approach to construct the FCOR maps. In this approach, the maps were continuously updated for each volume included in the analysis, leading to an improvement in the estimates of the FCOR values as the number of volumes increased. For the study involving ET patients, we used the entire resting-state fMRI data to construct the individual FCOR maps and compared these maps between patients and controls. We evaluated the FCOR maps associated with 14 well-known resting-state networks (Shirer et al., 2012) including the dorsal default mode network (dDMN), ventral default mode network (vDMN), precuneus network (Prec), anterior salience network (aSal), posterior salience network (pSal), right executive control network (RECN), left executive control network (LECN), visuospatial network (Visu), language network (Lang), basal ganglia network (BG), sensorimotor network (SMN), primary visual network (pVis), high visual network (hVis), and auditory network (Aud).

The reproducibility of FCOR maps across sessions as a function of the number of volumes included in generating the maps was evaluated using a similarity metric given by the following equation (Choe et al., 2015; Cohen et al., 2008):

$$\rho^2 = 1 - \frac{\sum_{i=1}^{V}[(a_i - m_i)^2 + (b_i - m_i)^2]}{\sum_{i=1}^{V}[(a_i - \overline{M})^2 + (b_i - \overline{M})^2]}$$

where a_i and b_i are values at voxel i in FCOR maps a and b, respectively, m_i is the mean value of the two maps at voxel i, $\overline{M}$ is the grand mean value across the mean image m, and V is the total number of voxels in the maps. Here a represents the FCOR map constructed using resting-state fMRI data acquired in session 1 and b the FCOR map for session 2. Note that the value of ρ^2 can vary from 0 to 1, with 0 indicating no similarity and 1 being identical.

Two-sample t-tests were used to compare differences in FCOR values across the whole brain (whole-brain comparisons) between patients and controls before and after MRgFUS treatment. We included age, sex, and mean frame-wise displacement (Power et al., 2014), representing head motion during resting-state fMRI scans, as covariates of no interest. Statistical significance was assessed using $p < 0.05$ corrected for multiple comparisons using family-wise error correction at the cluster level (FWEc) with a cluster-defining threshold (CDT) set at $p = 0.001$. In addition, we also performed statistical comparisons of FCOR values within the thalamus (within-thalamus comparisons) given the significant role of the thalamus in essential tremor.

(4) Region-of-interest analyses

We also performed several region-of-interest (ROI) analyses. Relevant regions that exhibited significant FCOR alterations in patients compared to controls were used as ROIs. FCOR values associated with the 14 resting-state networks were extracted from each ROI and the relationship between the extracted values and cognitive and motor function improvement scores were evaluated using a regression model with the FCOR values as the independent variable and the cognitive/motor improvement scores as dependent variables.

４．研究成果
(1) System performance

To investigate the feasibility of constructing FCOR maps in real-time, we evaluated the time to generate whole-brain FCOR maps from the preprocessed resting-state fMRI data. For this, we used a workstation running a Linux operating system with 754GB of memory and dual CPU each consisting of 24 cores running at 3.0GHz. The average time to update a whole-brain FCOR map per volume across all datasets was 0.12 s for aSal, 0.05s for Aud, 0.05s for BG, 0.20s for dDMN, 0.07s for hVis, 0.09s for Lang, 0.12s for LECN, 0.08s for pSal, 0.07s for Prec, 0.04s for pVis, 0.18s for RECN, 0.13s for SMN, 0.14s for vDMN, and 0.14s for Visu. The average time to compute the FCOR maps for all included resting-state networks was 1.48s per volume, below the TR = 2.5s, demonstrating the feasibility of constructing FCOR maps in real-time.

(2) Reproducibility of FCOR maps across imaging sessions

To quantify the reproducibility of the FCOR maps across sessions, we plotted in Figure **1** the behavior of the similarity metric of the different resting-state networks as a function of the number of volumes used to generate the maps. As can be seen from this figure, the similarity metric showed an initial exponential increase as the number of volumes increased, then plateaued as more volumes were added. To get a similarity value of 0.8, on average, the dDMN needed only 122 volumes (about 5 min of data at TR = 2.5s), whereas pVis needed 458 volumes (about 19 min of data at TR = 2.5s). The volumes needed for other networks were between these two values. Further increases in similarity require more volumes.
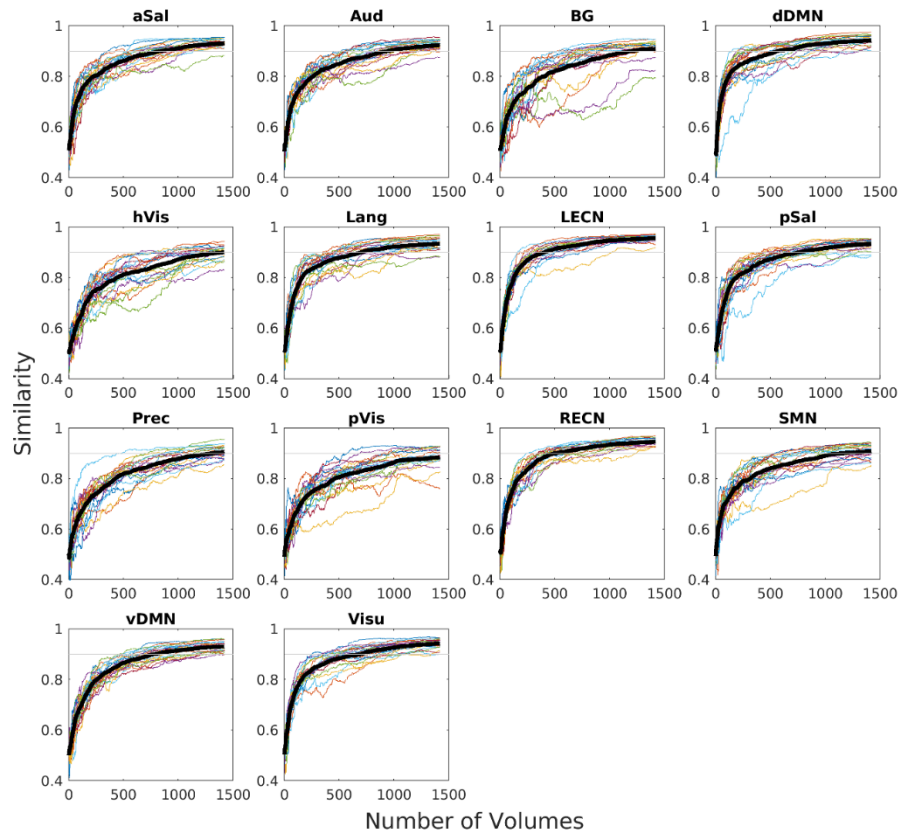
Figure 1. The value of the similarity metric as a function of the number of volumes used in constructing FCOR maps. Thick black lines represent the mean curve across all participants. Thin colored lines represent individual curves. The FCOR maps were constructed using correlation threshold equal to 0.1.
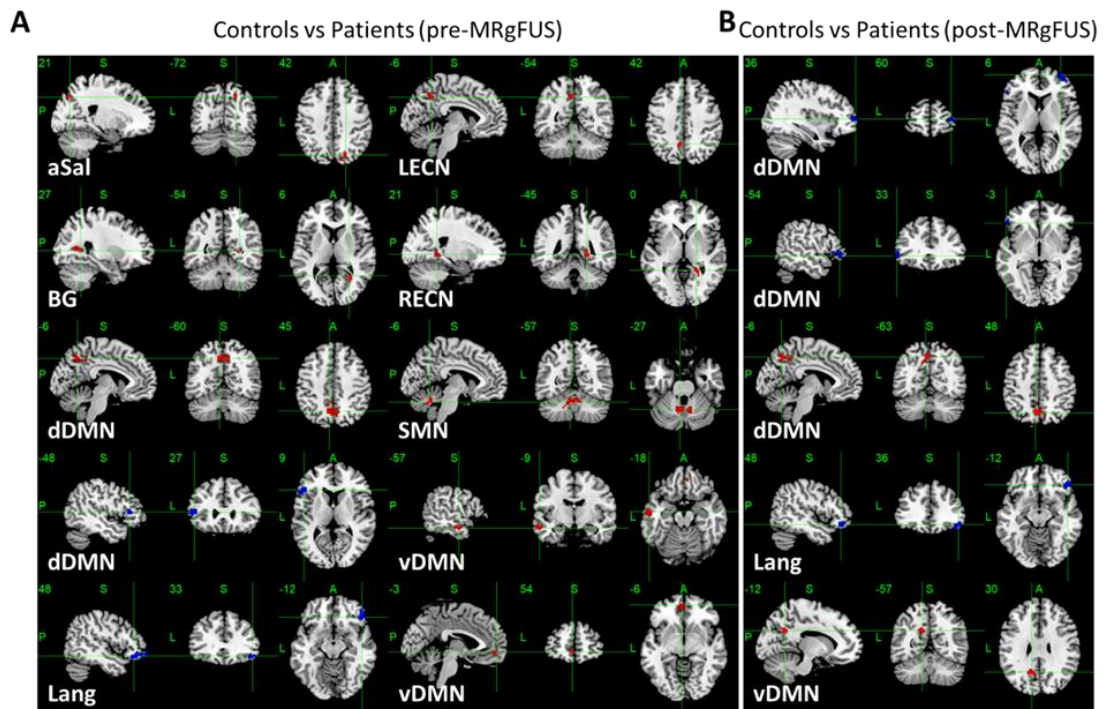

Figure 2. Comparison of whole-brain FCOR values between patients with essential tremor and healthy controls. Regions showing significant (FWEc p < 0.05, CDT p = 0.001) alterations in (A) pre-MRgFUS and (B) post-MRgFUS FCOR values for several resting-state networks are highlighted. Red indicates significantly higher FCOR values in patients, whereas blue indicates significantly lower FCOR values.

(3) FCOR alterations in patients with essential tremor

Comparison between patients and healthy controls showed several regions with significant alterations in FCOR values associated with several resting-state networks across the whole brain before and after

MRgFUS treatment (Figure **2**). Pre-operatively, the FCOR values of the superior parietal lobule with aSal, that of the precuneus with BG, dDMN, and LECN, that of the lingual gyrus with RECN, that of the middle temporal gyrus and medial frontal gyrus with vDMN, and that of the bilateral dentate nucleus (extending to the fastigium) in the cerebellum with SMN were significantly higher in patients compared to controls. By contrast, the FCOR values of the triangular and orbital part of the inferior frontal gyrus with dDMN and Lang, respectively, were significantly lower in the patient group. After MRgFUS treatment, most of the observed higher FCOR values in patients recovered to the same levels as controls, although a few clusters in the precuneus with significantly higher FCOR values with the default mode (dDMN, vDMN) and in the right middle frontal gyrus, left triangular part of the inferior frontal gyrus, and right orbital part of the inferior frontal gyrus with significantly lower FCOR values with dDMN and Lang networks were still observed (Figure **2**B). For the analyses within the thalamus, a cluster in the right pulvinar and an extended cluster in the left dorsomedial thalamus had widespread connections with hVis and SMN, respectively, in patients compared to controls before MRgFUS treatment. Postoperatively, the values recovered to healthy control levels. However, two closely spaced clusters, also in the dorsomedial thalamus just inferior to the one detected pre-operatively, showed significantly higher FCOR values with dDMN and vDMN. These two clusters were also close to the MRgFUS-target region in the ventral intermediate nucleus.

(4) Region-of-interest analyses using pre-MRgFUS FCOR values

From the different regions showing significant alterations in FCOR values in the patient group, we selected regions located in the cerebellum and thalamus for additional ROI analyses. The ROIs from the cerebellum corresponded to the bilateral dentate nucleus, denoted as LCer and RCer, and that from the thalamus corresponded to the pulvinar and dorsomedial nucleus, denoted as Th_hVis, Th_SMN, Th_vDMN, and Th_dDMN. Linear regression analyses showed that the FCOR values of LCer with LECN, pSal, RECN, and Visu were negatively associated (FDR p = 0.008, 0.010, 4.331×10^{-6}, and 3.171×10^{-9}, respectively) with ACE-R total score in patients, but not in controls. Moreover, in patients, the FCOR values of LCer with Visu were also negatively related with ACE-R's memory (FDR p = 0.001) and fluency (FDR p = 2.321×10^{-5}) sub-scores; the FCOR values of Th_dDMN with aSal, LECN, pSal, and Visu were associated with the attention sub-score (FDR p = 4.549×10^{-6}, 3.216×10^{-5}, 9.437×10^{-6}, and 3.332×10^{-6}, respectively); and the FCOR values of Th_dDMN with Visu were associated with the fluency sub-score (FDR p = 4.731×10^{-7}). Pre-MRgFUS FCOR values also showed association with motor function improvement scores as summarized in Figure **3**.
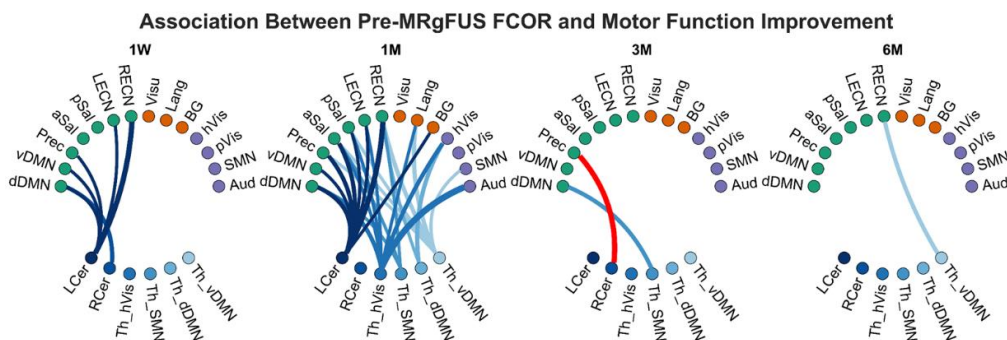

Figure 3. Influence of pre-MRgFUS FCOR values in the improvement of motor function after treatment. Pre-MRgFUS FCOR values of the shown connections between ROIs and the different resting-state networks have significant (FDR p < 0.05) negative linear relationship with motor function improvement score one week (1W), one month (1M), three months (3M), and six months (6M) after MRgFUS thalamotomy. Shades of blue distinguish different ROIs and their connections. Link thickness represents the strength of the relationship between FCOR values and motor function improvement scores.

(5) Summary of results

To summarize, our results demonstrated the feasibility of constructing FCOR maps in real-time (below TR) by utilizing a relatively high-performance computing system. Consistent with the principle of precision mapping, the reproducibility of the constructed FCOR maps also increased as more volumes were used to generate the maps. An application of FCOR analysis to investigate changes in whole-brain functional connectivity in patients with essential tremor showed altered FCOR values in multiple brain regions across several resting-state networks. Specifically, the dentate nucleus in the cerebellum and the dorsomedial thalamus showed widespread connections with SMN in patients compared to controls. In addition, the thalamic pulvinar also exhibited widespread connections with hVis in the patient group. The FCOR values of these regions with cognitive networks were also negatively associated with pre-operative cognitive and postoperative motor function improvement scores. Taken together, our findings suggest the feasibility of using FCOR to extensively evaluate brain network changes before, during (with real-time estimation), and after neurosurgical operations.

Epifanio Bagarinao, Satoshi Maesawa, Sachiko Kato, Manabu Mutoh, Yoshiki Ito, Tomotaka Ishizaki, Takafumi Tanei, Takashi Tsuboi, Masashi Suzuki, Hirohisa Watanabe, Minoru Hoshiyama, Haruo Isoda, Masahisa Katsuno, Gen Sobue, Ryuta Saito	121
Cerebellar and thalamic connector hubs facilitate the involvement of visual and cognitive networks in essential tremor	2024
Parkinsonism & Related Disorders	106034 106034
DOI 10.1016/j.parkreldis.2024.106034	

Kawabata Kazuya Bagarinao Epifanio Watanabe Hirohisa Maesawa Satoshi Mori Daisuke Hara Kazuhiro Ohdake Reiko Masuda Michihito Ogura Aya Kato Toshiyasu Koyama Shuji Katsuno Masahisa Wakabayashi Toshihiko Kuzuya Masafumi Hoshiyama Minoru Isoda Haruo Naganawa Shinji Ozaki Norio Sobue Gen	257
Functional connector hubs in the cerebellum	2022
NeuroImage	119263 119263
DOI 10.1016/j.neuroimage.2022.119263	

Yamamoto Maeri Bagarinao Epifanio Shimamoto Masanori Iidaka Tetsuya Ozaki Norio	35
Involvement of cerebellar and subcortical connector hubs in schizophrenia	2022
NeuroImage: Clinical	103140 103140
DOI 10.1016/j.nicl.2022.103140	

Kato Sanae Bagarinao Epifanio Isoda Haruo Koyama Shuji Watanabe Hirohisa Maesawa Satoshi Hara Kazuhiro Katsuno Masahisa Naganawa Shinji Ozaki Norio Sobue Gen	15
Reproducibility of functional connectivity metrics estimated from resting-state functional MRI with differences in days, coils, and global signal regression	2022
Radiological Physics and Technology	298 310
DOI 10.1007/s12194-022-00670-6	

Bagarinao Epifanio Kawabata Kazuya Watanabe Hirohisa Hara Kazuhiro Ohdake Reiko Ogura Aya Masuda Michihito Kato Toshiyasu Maesawa Satoshi Katsuno Masahisa Sobue Gen	4
Connectivity impairment of cerebellar and sensorimotor connector hubs in Parkinson's disease	2022
Brain Communications	fcac214
DOI 10.1093/braincomms/fcac214	

Kato Sachiko Maesawa Satoshi Bagarinao Epifanio Nakatsubo Daisuke Tsugawa Takahiko Mizuno Satomi Kawabata Kazuya Tsuboi Takashi Suzuki Masashi Shibata Masashi Takai Sou Ishizaki Tomotaka Torii Jun Mitoh Manabu Saito Ryuta Wakabayashi Toshihiko Katsuno Masahisa Ozaki Norio Watanabe Hirohisa Sobue Gen	138
Magnetic resonance-guided focused ultrasound thalamotomy restored distinctive resting-state networks in patients with essential tremor	2023
Journal of Neurosurgery	306 317
DOI 10.3171/2022.5.JNS22411	

Watanabe Hirohisa Bagarinao Epifanio Maesawa Satoshi Hara Kazuhiro Kawabata Kazuya Ogura Aya Ohdake Reiko Shima Sayuri Mizutani Yasuaki Ueda Akihiro Ito Mizuki Katsuno Masahisa Sobue Gen	13
Characteristics of Neural Network Changes in Normal Aging and Early Dementia	2021
Frontiers in Aging Neuroscience	747359 747359
DOI 10.3389/fnagi.2021.747359	

MAESAWA Satoshi BAGARINAO Epifanio NAKATSUBO Daisuke ISHIZAKI Tomotaka TAKAI Sou TORII Jun KATO Sachiko SHIBATA Masashi WAKABAYASHI Toshihiko SAITO Ryuta	62
Multitier Network Analysis Using Resting-state Functional MRI for Epilepsy Surgery	2022
Neurologia Medico-Chirurgica	45 55
DOI 10.2176/nmc.oa.2021-0173	

Maesawa Satoshi　Mizuno Satomi　Bagarinao Epifanio　Watanabe Hirohisa　Kawabata Kazuya　Hara Kazuhiro　Ohdake Reiko　Ogura Aya　Mori Daisuke　Nakatsubo Daisuke　Isoda Haruo　Hoshiyama Minoru　Katsuno Masahisa　Saito Ryuta　Ozaki Norio　Sobue Gen	15
Resting State Networks Related to the Maintenance of Good Cognitive Performance During Healthy Aging	2021
Frontiers in Human Neuroscience	753836　747359
DOI 10.3389/fnhum.2021.753836	

Kawabata Kazuya　Bagarinao Epifanio　Watanabe Hirohisa　Maesawa Satoshi　Mori Daisuke　Hara Kazuhiro　Ohdake Reiko　Masuda Michihito　Ogura Aya　Kato Toshiyasu　Koyama Shuji　Katsuno Masahisa　Wakabayashi Toshihiko　Kuzuya Masafumi　Hoshiyama Minoru　Isoda Haruo　Naganawa Shinji　Ozaki Norio　Sobue Gen	24
Bridging large-scale cortical networks: Integrative and function-specific hubs in the thalamus	2021
iScience	103106　103106
DOI 10.1016/j.isci.2021.103106	

		4	2	0

Epifanio Bagarinao
Impairments of connector hubs in brain disorders
25th Congress of Japan Human Brain Mapping Society
2023

Epifanio Bagarinao, Maeri Yamamoto, Masanori Shimamoto, Norio Ozaki
Schizophrenia significantly impacts the overall connectivity strength of brain hubs
44th Annual Meeting of the Japan Neuroscience Society
2021

O

	(Isoda Haruo) (40223060)	(33804)	
	(Maesawa Satoshi) (90566960)	(13901)	

O